Editorial Expression of Concern and Correction

APPLIED BIOLOGICAL SCIENCES

PNAS is publishing an Editorial Expression of Concern regarding the following article: "Use of combinatorial genetic libraries to humanize N-linked glycosylation in the yeast *Pichiapastoris*," by Byung-Kwon Choi, Piotr Bobrowicz, Robert C. Davidson, Stephen R. Hamilton, David H. Kung, Huijuan Li, Robert G. Miele, Juergen H. Nett, Stefan Wildt, and Tillman U. Gerngross, which appeared in issue 9, April 29, 2003, of *Proc Natl Acad Sci USA* (100:5022–5027; first published April 17, 2003; 10.1073/pnas.0931263100).

It has recently come to the attention of the editors that, since the time of submission to PNAS, patent protection and intellectual property issues have prevented the distribution of the yeast strains described in the above-noted article to qualified investigators. This is a violation of PNAS editorial policy and we are publishing this statement to alert readers. PNAS authors must ensure that all unique reagents described in their published paper are available to qualified researchers, and any restrictions on the sharing of materials must be disclosed to the editorial office at the time of submission (www.pnas.org/site/misc/iforc.shtml#viii).

Randy Schekman
Editor-in-Chief

NEUROSCIENCE

Correction for "Cortical activity during motor execution, motor imagery, and imagery-based online feedback," by Kai J. Miller, Gerwin Schalk, Eberhard E. Fetz, Marcel den Nijs, Jeffrey G. Ojemann, and Rajesh P. N. Rao, which appeared in issue 9, March 2, 2010, of *Proc Natl Acad Sci USA* (107:4430–4435; first published February 16, 2010; 10.1073/pnas.0913697107).

The authors note that, in the Acknowledgments, "National Institutes of Health Grant R01-61-3925" should read "National Institutes of Health Grants R01-61-3925, EB006356, and EB000856." Also, on page 4434, right column the equation appeared incorrectly.

$$A_{mr} = \frac{(\bar{m} - \bar{r})^3}{|\bar{m} - \bar{r}|\sigma_{mr}^2} \frac{N_m - N_r}{N_{m \cup r}^2}$$

should instead appear as

$$A_{mr} = \frac{(\bar{m} - \bar{r})^3}{|\bar{m} - \bar{r}|\sigma_{mr}^2} \frac{N_m * N_r}{N_{m \cup r}^2}.$$

This error does not affect the conclusions of the article.

EXPRESSION OF CONCERN

CORRECTION

Cortical activity during motor execution, motor imagery, and imagery-based online feedback

Kai J. Miller[a,b,1], Gerwin Schalk[c], Eberhard E. Fetz[a,d], Marcel den Nijs[b], Jeffrey G. Ojemann[e], and Rajesh P. N. Rao[a,f,1]

Departments of [a]Neurobiology and Behavior, [b]Physics, [d]Physiology and Biophysics, [e]Neurological Surgery, and [f]Computer Science and Engineering, University of Washington, Seattle, WA 98195; and [c]Wadsworth Center, New York State Department of Health, Albany, NY 12201

Imagery of motor movement plays an important role in learning of complex motor skills, from learning to serve in tennis to perfecting a pirouette in ballet. What and where are the neural substrates that underlie motor imagery-based learning? We measured electrocorticographic cortical surface potentials in eight human subjects during overt action and kinesthetic imagery of the same movement, focusing on power in "high frequency" (76–100 Hz) and "low frequency" (8–32 Hz) ranges. We quantitatively establish that the spatial distribution of local neuronal population activity during motor imagery mimics the spatial distribution of activity during actual motor movement. By comparing responses to electrocortical stimulation with imagery-induced cortical surface activity, we demonstrate the role of primary motor areas in movement imagery. The magnitude of imagery-induced cortical activity change was ~25% of that associated with actual movement. However, when subjects learned to use this imagery to control a computer cursor in a simple feedback task, the imagery-induced activity change was significantly augmented, even exceeding that of overt movement.

brain–computer interface | electrocorticography | primary motor cortex | learning | plasticity

Imagined motor movement ("imagery") has been shown to be crucial for motor skill learning in a variety of situations, ranging from learning new skills in sports (1) to overcoming the effects of neurological conditions (2, 3). Demonstration of residual cortical activity during imagery in motor areas in paraplegic individuals (4) and stroke victims (5) implies that motor imagery could play an important role in rehabilitation and prosthesis control (6). Because of this, many recent efforts to build "brain–computer interfaces" (BCIs) for paralyzed patients have relied on motor imagery to obtain volitional neural signals to control external devices (6–11).

Human brain imaging using hemodynamic markers (PET and fMRI) and extracerebral magnetic and electric field studies (MEG and EEG) have shown that motor imagery activates many of the same neocortical areas as those involved in planning and execution of motor movements (e.g., medial supplemental motor area, premotor cortex, dorsolateral prefrontal cortex, and posterior parietal cortex). The direct, population-scale, electrophysiologic correlate of these findings has not been quantified at the cortical surface. The relevance of primary motor cortex in motor imagery has remained an unresolved issue, there being evidence both supporting and against a role for primary motor areas during motor imagery (6, 12–19). Furthermore, the congruence of cortical electrophysiologic change associated with motor movement and motor imagery has not been determined.

Crone and colleagues, in 1998 (20), and others since then (21–24) have demonstrated that somatotopic motor function is revealed in the high frequencies of the cortical surface potential power spectral density (PSD). This cortical surface potential has been examined in humans with electrocorticography (ECoG), which employs the clinical placement of electrode arrays on the brain surface. Recent ECoG studies have demonstrated that these signals can characterize local cortical dynamics with very high spatiotemporal precision: for example, the independent

dynamics of individual fingers can be resolved at the 20-ms time scale in single electrodes (25). This is done by capturing noise-like, $1/f$, changes in the PSD of the cortical surface electrical potential (26), which directly correlate with population firing rate (27) and are plainly revealed at high frequencies (22, 25).

We apply ECoG to address the problem of imagery-associated cortical activity. As with EEG and MEG studies (17, 18), we find that, for a given movement type, the spatial distributions of motor-associated α and β rhythms (captured jointly here in an 8–32 Hz band) in lateral frontoparietal cortex overlap between overt movement and imagery. However, when comparing different movement types, we quantitatively show that these also overlap, demonstrating that the α/β-rhythm changes do not delineate local cortical function. In contrast, the spatial distribution of the high-frequency aspect of the ECoG signals does not overlap between movement types but does overlap between movement and imagery of the same type. This finding unambiguously establishes a shared representation for movement and imagery at the local population level. The role of primary motor areas in movement imagery was revealed by significant imagery-induced cortical surface activity at electrode sites where electrocortical stimulation produced movement. The magnitude of imagery-induced cortical activity was ~25% that of actual movement. When this same imagery was used to control a cursor in a simple feedback task, we found an augmentation of spatially congruent cortical activity, even beyond that found during movement.

Results

Movement. In an initial set of experiments, the subjects (Table S1) performed an interval-based task in which they alternated between several seconds of either hand or tongue movement and several seconds of rest in response to visual cues. We examined changes in the power spectral density (PSD) of the ECoG potential from all electrodes during and after the cue period. As in previous reports (20, 22, 23, 28), we found a spatially broad decrease in power in a low-frequency band (LFB) (8–32 Hz) and a spatially more focal increase in power in a broad high-frequency band (HFB) (76–100 Hz) during movement compared with rest (Figs. 1–3 and Figs. S1 and S2). The spatial distribution of activation was significantly overlapping between tongue movement and hand movement in the LFB [four of five subjects (Figs. 1 and 2 and Fig. S1; $P < 0.01$ by reshuffling—10^6 iterations, Fig. S3)], but not in the HFB (overlapping in one of five subjects).
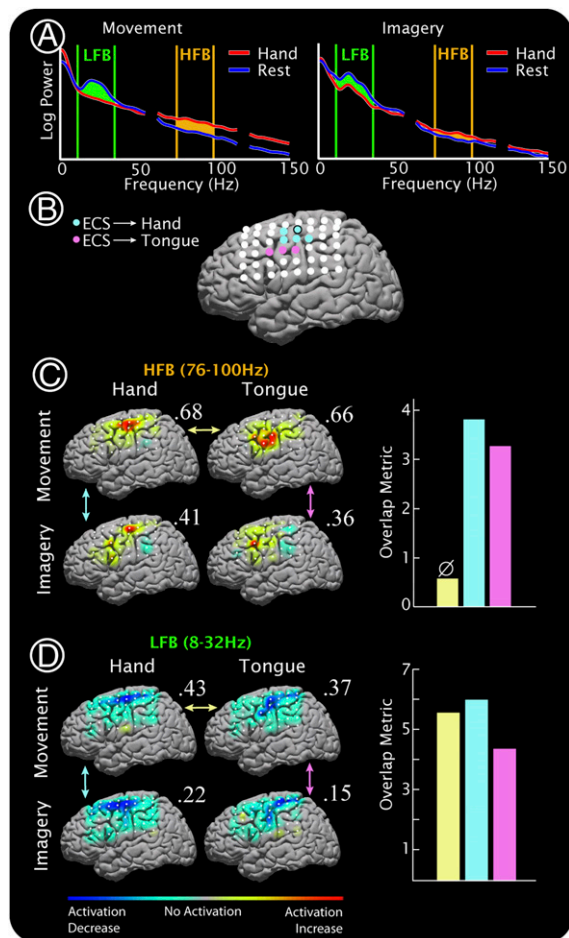
Fig. 1. Spectral changes in cortical surface potentials during hand and tongue movement and imagery in subject 1. (*A*) On the left, a characteristic example of the cortical potential power spectral density (PSD) for hand movement (red) and rest (blue) is shown. On the right, the same is seen between hand imagery (red) and rest (blue). The PSDs are from a primary motor electrode (Brodmann area 4, Talairach coordinate [−43, −14, 56], circled in *B*), referenced to the common average. Power at low frequencies ("LFB," 8–32 Hz, green) decreases with movement/imagery, and power at high frequencies ("HFB," 76–100 Hz, orange) increases during movement/imagery. In this electrode, the HFB increase with imagery is 32% that of movement (comparing orange areas). For the LFB, it is 90% (green areas). (*B*) The electrode positions are shown along with the electrodes in which stimulation produced movement of the hand (light blue) or tongue (light pink). The PSD in A is from the circled electrode. (*C*) Interpolated HFB activation maps for hand and tongue movement and imagery are shown on the left. Each is scaled to the maximum absolute value of activation (indicated by the number above each cortical map). On the right, the overlap is quantified between hand and tongue movement (yellow), hand movement and imagery (light blue), and tongue movement and imagery (light pink). ø, significance, *P* > 0.01 (by reshuffling, in this case *P* = 0.27). (*D*) As in *C*, for the LFB. All but the HFB hand movement vs. tongue movement comparison were significantly overlapping, with *P* < 10⁻⁴.

Imagery. The subjects then repeated the movement task, except that instead of moving they were instructed to kinesthetically imagine making that movement (19, 29) during the cue period (nonmovement verified by EMG, dataglove measurement, and observation; Fig. S4). In 4 of the 5 subjects who received electrocortical stimulation (ECS) as part of their clinical care, imagery produced a spatially focal, statistically significant (*P* < 0.05) increase in HFB power in electrodes where ECS produced movement of the same type (Figs. 1 and 4 and Figs. S1, S2, and S5). This confirms that primary motor areas are activated during imagery.
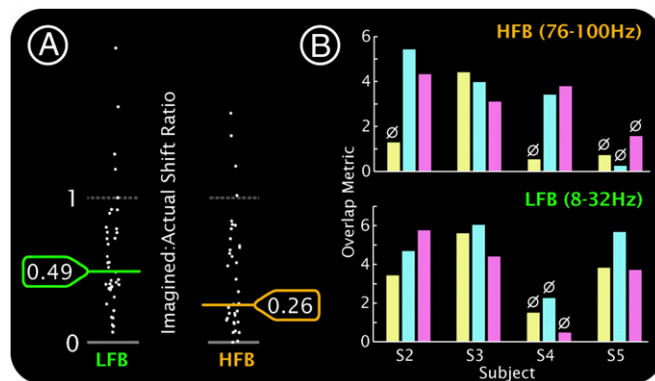

Fig. 2. Comparison of cortical activity during movement and imagery. (*A*) The plot shows the ratio of shift in power during imagery to that during movement for electrodes in which activity between movement and rest was significantly different. Each white dot indicates the ratio at an individual electrode. The geometric mean of the imagery:movement ratios for the HFB was 0.26. For the LFB it was 0.49 (LFB ratio was significantly larger than HFB ratio, *P* = 0.005 by permutation resampling, 10⁵ iterations). (*B*) For subjects 2–5, the overlap is quantified between hand and tongue movement (yellow), hand movement and imagery (light blue), and tongue movement and imagery (light pink). ø, significance, *P* > 0.01 (by reshuffling).

The spatially broad decrease in power in the LFB and spatially focal increase in power in the HFB were observed during imagery and were significantly overlapping with their movement counterparts, but the magnitudes of the spectral changes were smaller (Figs. 1, 2, 4, and 5 and Figs. S1, S2, S6, and S7). Across the 8 subjects, 38 electrodes were selected to quantify the magnitude of spectral change: those in which there was a significant difference in the PSD for both the HFB and LFB associated with movement (*P* < 0.05 *t* test, Bonferroni-corrected for the number of electrodes in that subject; 21 electrodes for tongue, 17 for hand). In these electrodes, the magnitude of spectral change in the HFB for imagery was 26% of that during actual movement (Fig. 2). For the LFB, the relative magnitude was 49%. The LFB change was significantly larger than the HFB change (*P* = 0.005 by permutation resampling, 10⁵ iterations).

The spatial overlap between movement and imagery was strong and significant across subjects in both the HFB [*P* < 0.05 in 13 of 14 cases, and *P* < 0.01 in 9 of 14 cases, by reshuffling (Fig. S3)] and the LFB (*P* < 0.05 in 11 of 14 cases and *P* < 0.01 in 9 of 14 cases). The movement–imagery overlap was not significantly different for the HFB than the LFB on a case-by-case basis (*P* = 0.60, *t* test of difference in overlap metric).

Feedback. Four subjects (S1, S2, S6, and S8) participated in an imagery-based learning task, in which the magnitude of cortical activation at a particular electrode was used to control a cursor on a screen during motor imagery. Based on the cortical changes seen in the simple movement/imagery tasks, amplitudes at particular electrodes and frequencies were chosen as features that controlled the speed and direction of 1-dimensional movement of a cursor on a computer screen (Fig. 3 and Fig. S8). Subjects rapidly (5–7 min) learned to accurately control the cursor by using motor imagery. In this feedback task, subject 1 attained 94% target accuracy using imagined word repetition (imagining repeating the word "move"); subject 2, 74%/90% with hand/tongue imagery; subject 6, 85% with shoulder imagery; and subject 8, 100% with tongue imagery. During this learning task, the spatial distribution of high-frequency ECoG activity was quantitatively conserved in each case, but the magnitude of the imagery-associated spectral change increased significantly (Figs. 3–5 and Figs. S6 and S7). In most cases, the spectral change associated with cursor control exceeded that observed during
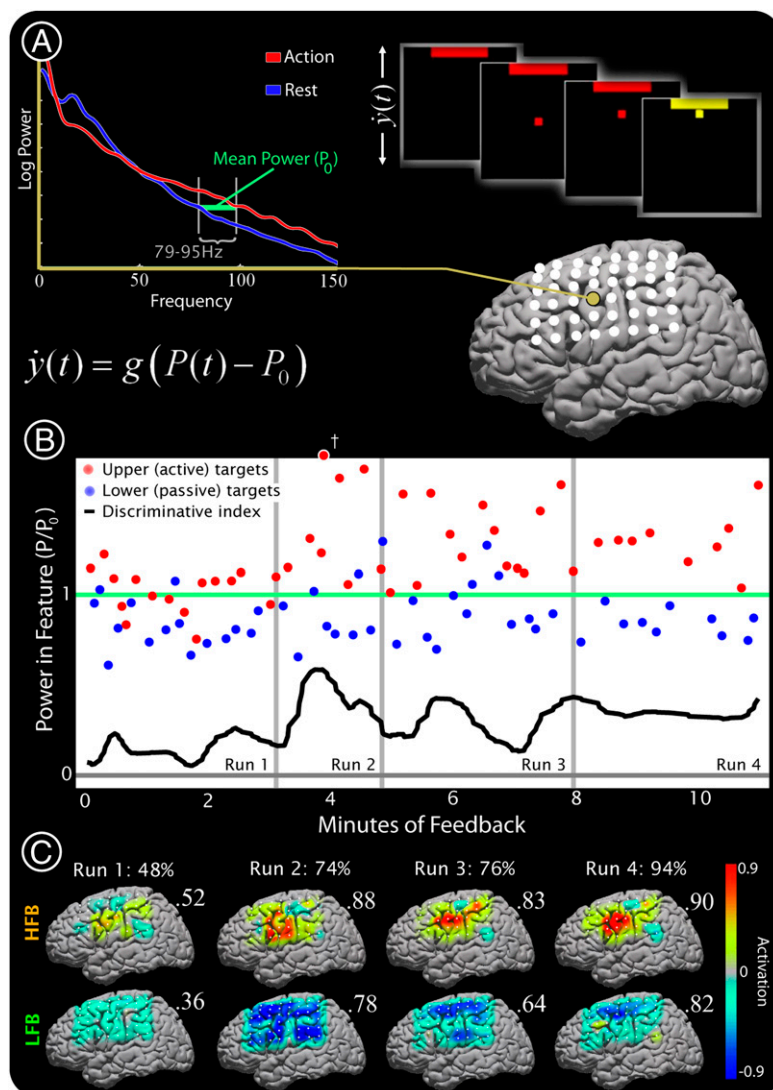
Fig. 3. Changes in cortical activity during feedback control of a cursor using ECoG in subject 1. (*A*) A specific electrode-frequency combination was identified from an initial motor task (gold electrode, 79–95 Hz; ECS-identified primary tongue cortex; see Fig. 1). The power, $P(t)$, in this feature was used to control the velocity of a computer cursor following the simple linear equation shown. The cursor velocity $\dot{y}$ was derived every 40 ms from the power $P(t)$ at the selected channel and frequency during the previous 280 ms (with respect to mean power, P_0). The subject was instructed to imagine saying the word 'move' to move the cursor toward one target ("active" target) and to rest (or "idle") to move the cursor to the other target ("passive" target). (*B*) The power at the chosen electrode-frequency combination is shown during four consecutive experimental runs of the cursor feedback task. Red dots indicate the mean power during active target trials, and blue dots indicate the mean power during passive target trials (datum noted with a cross represents an outlier lying beyond the upper edge of the plot). The green line denotes P_0, the mean power across passive/active trials. The black line indicates a "discriminative index"; i.e., the smoothed difference between the mean power during the previous three active target trials and the previous three passive target trials. This index demonstrates that target accuracies (shown in *C*) were highest when the subject found a middle dynamic range. After the third run, the subject reported having ceased to perform imagery, and instead "thought about the cursor moving up or down to get it to move" at some point during the run. (*C*) Distribution of HFB (upper brain plots) and LFB activations, as well as target hit accuracies (% next to run number), during each of the four experimental runs. All activation maps are to the same scale (indicated by the color bar). The final activations are most prominent at the electrode that was used for cursor control. The number flanking each brain plot is the maximum (absolute value) activation.

actual movement (4 of 5 cases in the HFB, 3 of 5 cases in the LFB). After several (5–8) minutes of training, subjects 1 and 6 reported that motor imagery ceased and was replaced by thinking about moving the cursor up or down.

Discussion

Similar to previous findings (20, 22, 23), we found a spatially broad decrease in power in the LFB (8–32 Hz) of the PSD during movement (Fig. 1), consistent with movement-induced desynchronization of the motor-associated frontoparietal α and β rhythms (30). With imagery, there is a similar, spatially broad, LFB

decrease that significantly overlaps that associated with the overt movement. This might have been anticipated from MEG- and EEG-based imagery studies that found similar patterns of desynchronization between movement and imagery (17, 18). However, as shown in Figs. 1 and 2 and Fig. S1, the spatial desynchronization pattern is very broad and significantly overlapping between different movement types on the cortical surface. This implies that the α/β desynchronization captured by our LFB, and measurable at the scalp surface, reflects an aspect of cortical processing that is fundamentally nonspecific. Rather than local, somatotopically distinct, population-scale computation, LFB
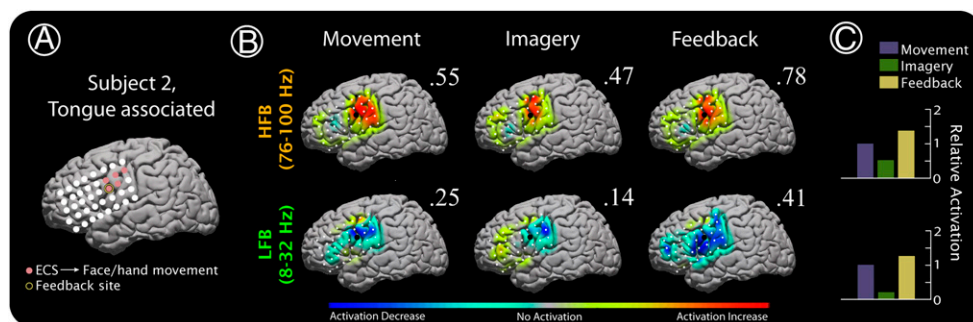
Fig. 4. Augmentation of cortical activity during learning in subject 2. (*A*) Electrocortical stimulation sites that produced face/hand movement (not further specified by neurologist) are shown. One of these (gold-circled) was selected from the motor/imagery tasks for feedback (using power from 37 to 43 Hz). (*B*) ECoG-based brain activation maps for tongue movement, imagined movement, and feedback-based BCI control of cursor, in the HFB and LFB ranges. Activation in each map is scaled to the maximum absolute activation (noted by flanking number). The feedback electrode is noted in each by an enlarged black dot. (*C*) Relative activation in the electrode-frequency combination for each of the conditions, computed by dividing the imagery- and feedback-related activation by the activation for actual movement, and normalizing the magnitude of activation for actual movement to 1 for all plots.

desynchronization may reflect something entirely different, such as altered feedback between cortical and subcortical structures (31–33), with a time scale of interaction that corresponds to the peak frequency in the PSD. The 50% LFB decrease in power during imagery might then represent only a partial "release" of cortex by subcortical structures (partial decoherence of a synchronized corticothalamic circuit; see Fig. 1*A*), compared with a more complete release during actual movement or after feedback.

In contrast, HFB (76–100 Hz) change is specific for different movement types. With movement, we see characteristic spatially focal increases in activity that are somatotopically specific: the resulting hand and tongue activation maps do not overlap (Figs. 1 and 2 and Fig. S1). The electrodes with statistically significant HFB change include primary motor cortical sites, where electrocortical stimulation (ECS; passing current between paired electrodes) produced corresponding hand or mouth movement. This HFB change is reflective of a broadband PSD increase that is obscured at lower frequencies by the motor-associated α/β rhythms (22). Indeed, choosing a wider frequency band for the HFB to capture more of this broadband change (extending well above 100 Hz) has been shown to produce the same result in motor cortex during movement (25, 34, 35). Through both simulation and experiment, this broadband change has been specifically correlated with local population firing rate (25–27, 36).

During hand or tongue imagery, there is a similar increase in HFB power relative to rest in a spatial distribution of electrodes that significantly overlaps with the movement-related distribution. Coupled with recent findings that suggest that PSD

amplitude changes linearly with neuronal firing rate (26, 27, 36), our finding of a 25% power increase with imagery, relative to movement, may imply that there is up to a 4-fold greater population firing rate during movement than imagery. Multiple mechanisms at the microcircuit level may be responsible for this. For example, a larger proportion of neurons in the population may be recruited during movement, of which only that subset that does not induce movement is active during imagery. This subset will not reflect the influence of recurrent somatic feedback, which is present during movement and absent during imagery. Given that motor imagery was recently shown to enhance corticospinal excitability (37), the 25% power increase may suggest that a subset of the neuronal population is activated during imagery, and that this subset "primes" the subset of neurons that send motor commands to the body. Alternately, the same population may be active throughout but with a higher firing rate in each neuron during movement or feedback. Recent work by Schieber and colleagues (38) showed that the relation between firing rate of single corticomotoneuronal cells and target muscle activity is not fixed but is context-dependent. This suggests that increases in the firing rate of large populations of motor cortical neurons may contribute to the HFB activity seen during imagery and feedback without inducing muscle contraction. Furthermore, although the precise relationship between fMRI-based BOLD activity and neuronal population activity is not straightforward (39), the ~25% HFB shift is similar to motor-imagery BOLD changes that were ~30% of those during movement (15).

Because the 1-cm spacing of the clinical ECoG array samples the cortical surface at roughly the scale of the somatotopic representation of different limbs in motor areas (40), this spacing is appropriate to reveal congruence in large-scale activation between motor imagery and overt movement, and imagery-based feedback. Our results show that these representations are quantitatively overlapping, suggesting that motor imagery involves the same distributed circuits as movement. The presence of imagery-based HFB spectral change in electrodes where electrocortical stimulation produces movement identifies a concrete role for primary motor cortex in imagery. The exposed cortical surface is sometimes dismissed as not belonging to primary motor cortex (i.e., that Brodmann area 4 is only within the bank of the central sulcus, and that only Brodmann area 6 is exposed and is a purely premotor region). This is a view that has been refuted: first, the Betz cells that define primary motor cortex can be found on the convexity of the precentral gyrus (41); second, the border of Brodmann area 4 extends rostrally to the vertex of the precentral gyrus (particularly dorsomedially) (42); and third, primary motor cortex can be robustly identified with ECS on the exposed precentral gyrus (43). In this context, our result cements the notion that motor imagery involves subliminal activation of the motor system (13) and also

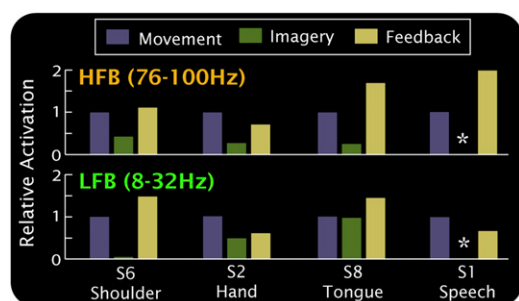**Fig. 5.** Relative activation for movement, imagery, and feedback in subjects S1, S2, S6, and S8, as in Fig. 3*C*. Subject 1 did not perform a speech (word repetition) imagery task. Together with the result of Fig. 3, the bar plots show that the magnitude of feedback imagery-related activation after learning is augmented, and, in four of five cases, exceeds the magnitude of activation for actual movement.

confirms that primary motor cortex is activated during motor imagery, validating claims by earlier noninvasive studies (16–19).

It has been known that the firing rate of single motor cortical neurons could be operantly conditioned with the help of explicit feedback (6, 44), and recent ECoG studies have demonstrated that imagery-associated feedback signals could be conditioned during a simple target task (8–11). Our study directly establishes that activity of widespread neuronal populations in motor cortex are augmented with simple imagery-based feedback (Figs. 3–5 and Fig. S6). The simplicity of this feedback task allows direct quantitative comparison with motor-associated representations. The dramatic augmentation, particularly in primary motor cortex, is significant because it demonstrates a dynamic restructuring of neuronal dynamics across whole populations in motor cortex, on very short time scales (<10 min).

Methods

Subjects. Simple motor and imagery tasks were studied in eight patients (two females, ages 12–48; Table S1) who underwent craniotomy and placement of peri-rolandic intracranial electrode arrays for 5–7 days to localize seizure foci before surgical treatment of medically refractory epilepsy. Array location and duration of implantation were determined solely by clinical criteria. Experiments were performed for 3–5 days at Children's Hospital (subject 6) and Harborview Hospital (all others) at the University of Washington. Subjects gave informed consent for participation, in a manner approved by the University of Washington Institutional Review Board.

Stimulation. In five of the eight patients (patients 1–4 and 7), electrocortical stimulation mapping (45, 46) of motor cortex was performed for clinical purposes. Each of these patients underwent stimulation mapping to identify motor and speech cortices as part of his/her clinical care. In this mapping, 5- to 10-mA square-wave current pulses (1 ms in length) were passed through paired electrodes for up to 3 s (or less if a response was evoked) to interrupt function, induce sensation, and/or evoke motor responses (Fig. S5). We denoted an electrode as a primary motor site if ECS produced simple movement.

Recordings. The platinum electrode arrays (Ad-Tech) were configured as 4×8 or 8×8-electrode grids. The electrode pads had 4-mm diameter (2.3 mm exposed) and 1-cm interelectrode distance, and were embedded in Silastic (Fig. S9). ECoG signals were split into two identical sets. One set was fed into the clinical EEG system (XLTEK), and the other set was recorded with Synamps2 (Neuroscan) biosignal amplifiers (Harborview Hospital; at 1,000 Hz) or g.USBamp (g.tec) amplifiers (Children's Hospital; at 1,200 Hz). ECoG signals were acquired from the experimental amplifiers using the general-purpose BCI2000 software (47), which was also used for online signal processing and stimulus presentation. The signals at Harborview Hospital were bandpass-filtered from 0.3 to 200 Hz. Surface EMG electrodes were placed for clinical purposes in a subset of patients (see Fig. S4 for illustration). Finger position was recorded during actual and imagined hand movement using a sensor dataglove (5DT) in a subset of patients (Fig. S4). Additionally, subjects were closely observed by experimenters for absence of movement during imagery, with brief pretask rehearsal with experimenter palpation.

Tasks. A series of three experiments were performed: interval-timed active motor movement, interval-timed motor imagery, and a cursor-to-target movement task to provide feedback on motor imagery. First, subjects performed simple, repetitive movements (22) of the hand (synchronous flexion and extension of all fingers; i.e., clenching and releasing a fist at a self-paced rate of ≈1 Hz), the tongue (opening of mouth with protrusion and retraction of the tongue; i.e., sticking the tongue in and out, also at 1 Hz), shoulder (shrug at 1Hz), or simple vocalization (saying the word "move"). These movements were performed in an interval-based fashion, alternating between 3-s movement blocks and rest. The side of actual or imagined somatic movement was always contralateral to the side of cortical grid placement. There were 30 text cues ("Hand," "Tongue," "Shrug," "Move") for each movement modality, delivered visually as text (2.5 cm high) at a distance of 75–100 cm from the subject. Cues of different type were interleaved randomly so no particular movement type could be anticipated.

Following the overt movement experiment, each subject performed an imagery task, imagining making identical movement rather than executing the movement. The imagery was kinesthetic rather than visual (19, 29) ("imagine yourself performing the actions like you just did"; i.e., "don't imagine what it looked like, but imagine making the motions").

One half of the subjects (1, 2, 6, 8) also performed an imagery-based brain–computer interface task (the others did not because clinical conditions limited the time available for participation in our experiments). The activation (A_{mr}; see below) was calculated in 2-Hz bins at each electrode, from the basic motor or imagery task. Experimenters then visually selected a feedback feature, a particular electrode and frequency combination, to be used for online cursor control. That frequency-range power from a particular electrode was coupled to the speed of a computer cursor using a simple linear relation (Fig. 5). Targets were presented in random order, in one of two locations on the periphery of the screen (e.g., up/down or left/right). The subject was instructed to imagine (again, via kinesthetic imagery) a particular movement to move a cursor toward one target (the "active" direction), and to rest (or "idle") to move the cursor to the other target (the "passive" direction). The active and passive targets were presented in a block-randomized fashion, and in approximately equal numbers. A trial was terminated when the cursor hit any target or when movement time exceeded a fixed duration (7.2 s). A trial was followed by a 1-s "reward" period during which the target turned yellow if the correct target was hit. The reward period was followed by a 1-s rest period during which the screen was blank before the next trial began. A trial was considered a "miss" if the wrong target was hit or the timeout length was reached. Targets were presented continuously for ∼2 min (i.e., a run), and the experiment typically consisted of three to five such runs.

Signal Analysis. A high-frequency band (HFB) (76–100 Hz) and a low-frequency band (LFB) (8–32 Hz) were chosen for analysis, as described in previous studies (22). This LFB range was chosen to capture the full width of motor-associated α/β rhythm spectral change, as well as variability in the peak of the motor rhythm, across brain areas and subjects (35). Samples of the power spectrum were compared between movement and rest in the movement task, imagery and rest in the imagery task, and upper targets and lower targets in the feedback task (illustrated in Fig. S10). During mixed hand–tongue tasks, hand (tongue) movement cues were compared only to rest cues following hand (tongue) movement because the beta rebound following movement is task-specific (30). The cursor velocity was determined online each 40 ms based on the power in a particular frequency range/electrode combination calculated over the prior 280 ms.

ECoG "activation," A_{mr}, was quantified as

$$A_{mr} = \frac{(\bar{m} - \bar{r})^3}{|\bar{m} - \bar{r}|\sigma_{mr}^2} \frac{N_m - N_r}{N_{m\cup r}^2},$$

where m denotes distribution of samples of power (with mean $\bar{m}$) for movement/imagery/active-feedback cues and r denotes distribution of power for rest/idling/passive-feedback target cues. The combined (joint) distribution is denoted $m\cup r$. N_m and N_r are the number of samples of type m, r, respectively, and $N_{m\cup r} = N_m + N_r$. A_{mr} is essentially the signed squared cross-correlation coefficient (r^2) comparing two distributions of the normalized power in the ECoG HFB or LFB. In other words, A_{mr} is the percentage of the variance in the data that can be explained by the fact that two subdistributions m and r have different means, $\bar{m}$ and $\bar{r}$, with an attached sign to indicate whether an increase or decrease associated with the action (vs. rest). The imagery:movement ratio is $\bar{m} - \bar{r}$ for imagery, divided by $\bar{m} - \bar{r}$ for movement in the same electrode.

To quantify power shift during feedback, the ratios of the activation metrics, A_{mr}, were used instead, because the trial numbers and durations were not balanced, and a statistical measure was considered to be more appropriate. However, the values of the resulting ratios involving feedback are considered meaningful only in the sense that one case is larger than another.

The overlap metric and overlap significance between patterns of brain activation were determined using a reshuffling technique (illustrated in Fig. S3). The dot product of the activations between two cases was determined (e.g., $\sum_k A_{mr}(e_k; \text{Imagery}) \times A_{mr}(e_k; \text{Movement})$, where e_k denotes the kth electrode).

Then, a distribution of surrogate overlap dot-products was generated by randomly reshuffling the channel labels for the imagery task, and then recomputing. The associated overlap metric was the value of the appropriate dot product in z-score units from the surrogate distribution. The associated P value was the probability that a surrogate dot product value was larger than the actual dot product.

Electrode Localization and Template Brain Mapping. Electrode locations were estimated based upon their relation to skull table and landmarks from the sagittal (lateral) and coronal (anterior-posterior) skull x-rays using the LOC package (48).

We also used this package to plot electrode locations and spatial distribution of activity on the AFNI-MNI template brain. ECoG activation maps were created for the HFB and LFB independently in each patient, for each task. We created these maps by linear superposition of activation, weighted by spherical Gaussian kernels (standard deviation of 5 mm) centered at the location of each electrode, and interpolated the superposition at each point in a template brain (Fig. S10).

1. Murphy SM (1994) Imagery interventions in sport. *Med Sci Sports Exerc* 26:486–494.
2. Dijkerman HC, Ietswaart M, Johnston M, MacWalter RS (2004) Does motor imagery training improve hand function in chronic stroke patients? A pilot study. *Clin Rehabil* 18:538–549.
3. Page SJ, Levine P, Leonard A (2007) Mental practice in chronic stroke: results of a randomized, placebo-controlled trial. *Stroke* 38:1293–1297.
4. Alkadhi H, et al. (2005) What disconnection tells about motor imagery: evidence from paraplegic patients. *Cereb Cortex* 15:131–140.
5. Sharma N, Pomeroy VM, Baron JC (2006) Motor imagery: a backdoor to the motor system after stroke? *Stroke* 37:1941–1952.
6. Hochberg LR, et al. (2006) Neuronal ensemble control of prosthetic devices by a human with tetraplegia. *Nature* 442:164–171.
7. Kübler A, Birbaumer N (2008) Brain-computer interfaces and communication in paralysis: extinction of goal directed thinking in completely paralysed patients? *Clin Neurophysiol* 119:2658–2666.
8. Leuthardt EC, Schalk G, Wolpaw JR, Ojemann JG, Moran DW (2004) A brain-computer interface using electrocorticographic signals in humans. *J Neural Eng* 1:63–71.
9. Leuthardt EC, Miller KJ, Schalk G, Rao RP, Ojemann JG (2006) Electrocorticography-based brain computer interface—the Seattle experience. *IEEE Trans Neural Syst Rehabil Eng* 14:194–198.
10. Schalk G, et al. (2008) Two-dimensional movement control using electrocorticographic signals in humans. *J Neural Eng* 5:75–84.
11. Felton EA, Wilson JA, Williams JC, Garell PC (2007) Electrocorticographically controlled brain-computer interfaces using motor and sensory imagery in patients with temporary subdural electrode implants. Report of four cases. *J Neurosurg* 106:495–500.
12. Naito E, et al. (2002) Internally simulated movement sensations during motor imagery activate cortical motor areas and the cerebellum. *J Neurosci* 22:3683–3691.
13. Jeannerod M, Frak V (1999) Mental imaging of motor activity in humans. *Curr Opin Neurobiol* 9:735–739.
14. de Lange FP, Roelofs K, Toni I (2008) Motor imagery: a window into the mechanisms and alterations of the motor system. *Cortex* 44:494–506.
15. Porro CA, et al. (1996) Primary motor and sensory cortex activation during motor performance and motor imagery: a functional magnetic resonance imaging study. *J Neurosci* 16:7688–7698.
16. Roth M, et al. (1996) Possible involvement of primary motor cortex in mentally simulated movement: a functional magnetic resonance imaging study. *Neuroreport* 7:1280–1284.
17. Schnitzler A, Salenius S, Salmelin R, Jousmäki V, Hari R (1997) Involvement of primary motor cortex in motor imagery: a neuromagnetic study. *Neuroimage* 6:201–208.
18. McFarland DJ, Miner LA, Vaughan TM, Wolpaw JR (2000) Mu and beta rhythm topographies during motor imagery and actual movements. *Brain Topogr* 12:177–186.
19. Guillot A, et al. (2009) Brain activity during visual versus kinesthetic imagery: an fMRI study. *Hum Brain Mapp* 30:2157–2172.
20. Crone NE, Miglioretti DL, Gordon B, Lesser RP (1998) Functional mapping of human sensorimotor cortex with electrocorticographic spectral analysis. II. Event-related synchronization in the gamma band. *Brain* 121:2301–2315.
21. Ball T, Schulze-Bonhage A, Aertsen A, Mehring C (2009) Differential representation of arm movement direction in relation to cortical anatomy and function. *J Neural Eng* 6:016006.
22. Miller KJ, et al. (2007) Spectral changes in cortical surface potentials during motor movement. *J Neurosci* 27:2424–2432.
23. Aoki F, Fetz EE, Shupe L, Lettich E, Ojemann GA (1999) Increased gamma-range activity in human sensorimotor cortex during performance of visuomotor tasks. *Clin Neurophysiol* 110:524–537.
24. Kubánek J, Miller KJ, Ojemann JG, Wolpaw JR, Schalk G (2009) Decoding flexion of individual fingers using electrocorticographic signals in humans. *J Neural Eng* 6:066001.

25. Miller KJ, Zanos S, Fetz EE, den Nijs M, Ojemann JG (2009) Decoupling the cortical power spectrum reveals real-time representation of individual finger movements in humans. *J Neurosci* 29:3132–3137.
26. Miller KJ, Sorensen LB, Ojemann JG, den Nijs M (2009) Power-law scaling in the brain surface electric potential. *PLOS Comput Biol* 5:e1000609.
27. Manning JR, Jacobs J, Fried I, Kahana MJ (2009) Broadband shifts in local field potential power spectra are correlated with single-neuron spiking in humans. *J Neurosci* 29:13613–13620.
28. Crone NE, et al. (1998) Functional mapping of human sensorimotor cortex with electrocorticographic spectral analysis. I. Alpha and beta event-related desynchronization. *Brain* 121:2271–2299.
29. Neuper C, Scherer R, Reiner M, Pfurtscheller G (2005) Imagery of motor actions: differential effects of kinesthetic and visual-motor mode of imagery in single-trial EEG. *Brain Res Cogn Brain Res* 25:668–677.
30. Pfurtscheller G (1999) *Event-Related Desynchronization (ERD) and Event Related Synchronization (ERS)* (Williams and Wilkins, Baltimore).
31. Schnitzler A, Timmermann L, Gross J (2006) Physiological and pathological oscillatory networks in the human motor system. *J Physiol (Paris)* 99:3–7.
32. Brown P (2003) Oscillatory nature of human basal ganglia activity: relationship to the pathophysiology of Parkinson's disease. *Mov Disord* 18:357–363.
33. Feige B, et al. (2005) Cortical and subcortical correlates of electroencephalographic alpha rhythm modulation. *J Neurophysiol* 93:2864–2872.
34. Miller KJ, et al. (2007) Real-time functional brain mapping using electrocorticography. *Neuroimage* 37:504–507.
35. Miller KJ, et al. (2008) Beyond the gamma band: the role of high-frequency features in movement classification. *IEEE Trans Biomed Eng* 55:1634–1637.
36. Whittingstall K, Logothetis NK (2009) Frequency-band coupling in surface EEG reflects spiking activity in monkey visual cortex. *Neuron* 64:281–289.
37. Li S, Stevens JA, Rymer WZ (2009) Interactions between imagined movement and the initiation of voluntary movement: a TMS study. *Clin Neurophysiol* 120:1154–1160.
38. Davidson AG, Chan V, O'Dell R, Schieber MH (2007) Rapid changes in throughput from single motor cortex neurons to muscle activity. *Science* 318:1934–1937.
39. Logothetis NK (2008) What we can do and what we cannot do with fMRI. *Nature* 453:869–878.
40. Woolsey CN, Erickson TC, Gilson WE (1979) Localization in somatic sensory and motor areas of human cerebral cortex as determined by direct recording of evoked potentials and electrical stimulation. *J Neurosurg* 51:476–506.
41. Rivara CB, Sherwood CC, Bouras C, Hof PR (2003) Stereologic characterization and spatial distribution patterns of Betz cells in the human primary motor cortex. *Anat Rec* 270A:137–151.
42. Geyer S, Matelli M, Luppino G, Zilles K (2000) Functional neuroanatomy of the primate isocortical motor system. *Anat Embryol (Berl)* 202:443–474.
43. Suess O, Suess S, Brock M, Kombos T (2006) Intraoperative electrocortical stimulation of Brodman area 4: a 10-year analysis of 255 cases. *Head Face Med* 2:20.
44. Fetz EE (1969) Operant conditioning of cortical unit activity. *Science* 163:955–958.
45. Ojemann G, Ojemann J, Lettich E, Berger M (1989) Cortical language localization in left, dominant hemisphere. An electrical stimulation mapping investigation in 117 patients. *J Neurosurg* 71:316–326.
46. Ojemann GA (1982) Models of the brain organization for higher integrative functions derived with electrical stimulation techniques. *Hum Neurobiol* 1:243–249.
47. Schalk G, McFarland DJ, Hinterberger T, Birbaumer N, Wolpaw JR (2004) BCI2000: a general-purpose brain-computer interface (BCI) system. *IEEE Trans Biomed Eng* 51:1034–1043.
48. Miller KJ, et al. (2007) Cortical electrode localization from X-rays and simple mapping for electrocorticographic research: The "Location on Cortex" (LOC) package for MATLAB. *J Neurosci Methods* 162:303–308.

NEUROSCIENCE